Journal of
Materials Chemistry B

Accepted Manuscript

This article can be cited before page numbers have been issued, to do this please use: A. Zhang, W. Wu, C. Zhang, Q. Wang, Z. Zhuang, H. Cheng and X. Zhang, *J. Mater. Chem. B*, 2019, DOI: 10.1039/C8TB03094D.

ROYAL SOCIETY OF CHEMISTRY

rsc.li/materials-b

ROYAL SOCIETY OF CHEMISTRY
View Article Online
DOI: 10.1039/C8TB03094D

Journal Name

ARTICLE

A Versatile Bacterial Membrane-Binding Chimeric Peptide with Enhanced Photodynamic Antimicrobial Activity

Received 00th January 20xx,
Accepted 00th January 20xx

DOI: 10.1039/x0xx00000x

www.rsc.org/

Ai-Nv Zhang,‡[a] Wei Wu,‡[b] Chi Zhang,[b] Qiu-Yang Wang,[b] Ze-Nan Zhuang,[b] Han Cheng,*[b] and Xian-Zheng Zhang*[b]

Photodynamic therapy (PDT) has become an effective antibiosis method for overcoming antibiotic resistance. In this study, we developed a versatile bacterial membrane-binding chimeric peptide PpIX-[PEG_8-$(KLAKLAK)_2$]$_2$ (denoted as PPK) by conjugating a photosensitizer protoporphyrin IX (PpIX) with the antimicrobial peptide $(KLAKLAK)_2$ (KLA) for effective photodynamic inactivation of bacteria. The chimeric peptide PPK with positively charged property and α-helical conformation could rapidly bind to microbial cells through electrostatic interaction and membrane insertion. Moreover, PPK could disrupt bacterial membrane and further elicit lipid bilayer leakage to kill bacteria by toxic reactive oxygen species (ROS) generated by PpIX under 660 nm light. *In vitro* experiments demonstrated that cationic PPK possessed excellent antimicrobial activity against both Gram-positive bacteria *Staphylococcus aureus* (*S. aureus*) and Gram-negative bacteria *Escherichia coli* (*E. coli*). Afterward, PPK also exhibited perfect therapeutic effects on *S. aureus*-infected mice without any systemic side effect. This chimeric peptide PPK will find great potential for photodynamic antibiosis.

1. Introduction

appropriate. Antibiotic resistance owing to inappropriate prescriptions or long-term abuse of antibiotics has become a worldwide health problem. Consequently, a significant level of attention is now received by peptide-based antibacterial agents.[1] Most conventional antibiotics (such as amikacin, doxycycline and ceftazidime) penetrate into bacteria and exert the antibacterial potential by inducing the breakage of DNA, hampering the cell division and triggering the release of intrinsic autolysins. However, these bacteria could easily develop resistance based on the tough and unbreakable bacterial wall.[2] For example, *E. coli* with the intact morphology could develop resistance to most available antibiotics.[3] Thus, there is an urgent need to develop novel alternative antimicrobial materials, which can effectively kill bacteria without inducing bacterial resistance. To date, several non-antibiotic materials have been proposed to inhibit bacteria, such as metal or metal oxide nanoparticles,[4,5] graphene-based materials,[6] antimicrobial peptides[7] and photosensitizers (PSs).[8-12]

Among the alternative antimicrobial materials, PSs as effective photodynamic therapeutic agents can be excited by visible light with suitable wavelength to generate toxic reactive oxygen species (ROS) in the presence of oxygen.[13] The photo-activated ROS via energy or electron transfer mechanisms is capable of irreversibly damaging bacterial membrane, protein, endoenzyme and DNA, resulting in the death of bacteria by a complex cascade of biological and physiological reactions.[14] Unlike common sanitizers, ROS are environmentally friendly for their short life (0.03 to 0.18 ms) and small radius (< 0.02 μm).[15] And it has been shown that photodynamic therapy (PDT) has significant advantages over the antibiotic-based conventional therapy with a promising antibiosis potential.[16,17]

Currently, a wide variety of anionic and neutral PSs have been used to effectively eliminate Gram-positive bacteria with promising effects,[18,19] whereas Gram-negative bacteria are less susceptible to the same treatment.[20] The resistance of Gram-negative bacteria to various PSs is owing to the presence of a relatively impermeable barrier (such as phospholipids, lipopolysaccharides (LPS), lipoteichoic acids and lipoproteins), which can restrict the photodynamic effects of PSs by impeding the interaction between the toxic ROS and bacteria.[21] In addition, PSs are often hydrophobic and are prone to aggregating in physical media, leading to the ineffectiveness of ROS.[22] Thus, many approaches were proposed to enhance the solubility and affinity of PSs, such as polylysine, polyethyleneimine, lipopolysaccharide,[23-25] membrane disrupting agents (EDTA)[26,27] and antibiotics.[28]

In this study, a bacterial membrane-binding chimeric peptide PPK was designed for treatment of bacterial infection. As shown in Scheme 1, PPK was mainly constructed with three components: 1) Cationic charged KLA to promote the affinity of PPK with negative charged microbial cell surface through electrostatic interaction or membrane insertion; 2)

[a] College of Pharmacy, Hubei University of Medicine, Shiyan 442000, P. R. China.
[b] Key Laboratory of Biomedical Polymers of Ministry of Education & Department of Chemistry, Wuhan University, Wuhan 430072, P. R. China.
Electronic Supplementary Information (ESI) available: Detailed synthesis process, ESI-MS of KLA and PPK, additional H&E-stained tissue sections from major organs, hemolysis of KLA, PpIX and PPK, hematologic analysis of post-injection mice. See DOI: 10.1039/x0xx00000x
*Corresponding authors: chm128256@163.com (H. C.), xz-zhang@whu.edu.cn (X. Z. Z.)
‡ The first two authors contributed equally to this paper.

View Article Online
DOI: 10.1039/C8TB03084B

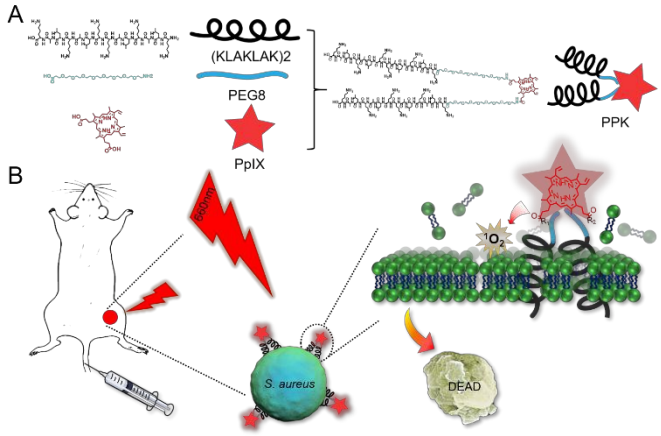

Scheme 1. Schematic illustration of the molecular structure of the chimeric peptide PPK and its antibacterial mechanism via bacterial membrane binding and damaging. A) The positive-charged chimeric peptide PPK was comprised of the positively charged and α-helical proapoptotic peptide KLA, the hydrophilic PEG_8 and the photosensitizer PpIX. B) The chimeric peptide PPK with positively charged property and α-helical conformation could rapidly bind to the bacterial membrane through electrostatic interaction and membrane insertion. Then the antibacterial effect was achieved by the toxic ROS generation at the bacterial membrane domain under 660 nm light.

polyethylene glycol (PEG) linker to enhance the biocompatibility and prolong blood circulation;[29,30] 3) photosensitizer PpIX with efficient ROS generation for potential PDT. Once accumulated at the bacterial membrane surface, PPK could disrupt bacteria cell membrane, causing liposomal leakage and oxidation of nucleic acids with the generation of ROS upon 660 nm light. Both *in vitro* and *in vivo* experiments were carried out to measure the photodynamic inactivation of bacteria by the use of PPK.

2. Materials and methods

2.1. Material preparation and characterization

2.1.1. Materials. Fmoc-D-Lys(Boc)-OH, Fmoc-D-Leu-OH, Fmoc-D-Ala-OH, 1-hydroxybenzotriazole (HOBt), 2-Chlorotrityl chloride resin and HBTU were purchased from GL Biochem. Ltd (Shanghai). Fmoc-PEG_8-COOH was provided by Zhoubei Technology Co. Ltd. (Hangzhou, China). Trifluoroacetic acid (TFA), triisopropylsilane and protoporphyrin were purchased from Aladdin-Reagent Co. Ltd (China). N,N-dimethylformamide (DMF) was provided by Shanghai chemical Co. Ltd (Shanghai, China) and distilled prior to use. All other reagents were from Shanghai chemical Co. Ltd (Shanghai, China). 2',7'-dichlorofluorescin diacetate (DCFH-DA) was provided by Beyotime Institute of Biotechnology (China). Live/dead backlight bacterial viability was purchased from Thermo Fisher Scientific. Luria-Bertani (LB) broth and LB Agar were purchased from Guangdong Huankai Microbial Sci. & Tech. Co. Ltd (Guangdong, China). *Staphylococcus aureus* (CMCC (B) 26003) and *Escherichia coli* (*E. coli*, strain MG1655) strains were obtained from the American Type Culture Collection (ATCC).

2.1.2 Synthesis of peptides. PpIX-[PEG-$(KLAKLAK)_2]_2$ and KLA were synthesized as our previous report.[31] Briefly, peptide sequence was linked to 2-chlorotriyl chloride resin (0.939 mmol g^{-1}). The peptide was cleaved from resin with a cleavage cocktail of trifluoroacetic acid (TFA), DI water and triisopropylsilane in the volume ratio of 95:2.5:2.5 for 1.5 h. The filtration was concentrated to a viscous solution by rotary evaporation. After the precipitation in cold ether, the crude product was dialyzed in a dialysis bag with molecular weight 1000 Da against ultrapure water for 24 h. The dialyzed PPK suspension was freeze-dried. The molecular weight of the peptides was determined by ESI-MS (Finnigan LCQ advantage). The obtained PPK and KLA were dissolving by PBS, and PpIX was dissolving in dimethyl sulfoxide (DMSO, 0.1% v/v). All the solutions were filtered-sterilized and stored at 4 °C in the dark for subsequent experiments.

2.1.3 UV-vis. UV-vis absorption spectra were measured in water on a Perkin-Elmer Lambda 45 UV-vis spectrophotometer with 1 cm path length quartz cuvettes.

2.1.4 FT-IR. FT-IR analysis was performed by a Perkin Elmer spectrophotometer by pressing corresponding samples into KBr pellet.

2.1.5 Detection of ROS in solution. Endogenous ROS was quantified by fluorescence spectroscopy using 2',7'-dichlorfluorescein-diacetate (DCFH-DA). Briefly, freshly prepared PPK (final concentration 200 μM) was mixed with DCFH-DA (final concentration 10 μM) under 660 nm light (30 mW/cm^2, 10 min). The fluorescence of 2',7'-dichlorofluoroscein (DCF) at 485 nm was recorded every 10 s to monitor the enhancement of fluorescence.

2.2. Bacteria culture and *in vitro* antimicrobial assay

2.2.1 Bacteria culture. The bacterial strains used in this study were *S. aureus* and *E. coli* MG1655. Glycerol stocks were established for each strain until being used in subsequent experiments. Fresh cultures were inoculated with dilution of 1:1000 and cultured with Luria-Bertani broth (LB) in 15 mL round-bottom Falcon culture tubes. The cells were grown under aerobic conditions at 37 °C in a shaking incubator for overnight. The cells in the mid log phase (OD_{600}~0.4-0.6) were harvested and diluted to a concentration of 1~2×10^5 CFU/mL (the optical density (OD) of the bacterial was measured at 600 nm using a microplate readers).

2.2.2 Antimicrobial assay. *S. aureus* and *E. coli* (1×10^5 CFU/mL) were mixed with KLA, PpIX and PPK at a concentration of 0.1, 1, 5 and 10 μM, respectively. Cultured bacteria (*E. coli* and *S. aureus*) were kept in dark and incubated at 37 °C for 30 min, then PpIX and PPK group were taken a light (30 mW/cm^2, 660 nm) for 10 min. After that, all solutions were immediately removed and serially diluted 100 fold, and each diluted solution was plated on LB agar plate for overnight incubation at 37 °C. All measurements were the average of 3 independent experiments. Colony forming unit (CFU) was counted to estimate the inhibition rate of bacterium. The minimum bactericidal concentration (MBC) was defined as the minimal peptide concentration that completely inhibited bacterial growth.

2.2.3 Confocal laser-scanning microscopy (CLSM). *S. aureus* and *E. coli* in mid-logarithmic phase were harvested by

View Article Online
DOI: 10.1039/C8TB03094D

centrifugation (590 g, 5min), washed three times and re-suspended in PBS to a concentration of 1×10^5 CFU/mL. PPK and PpIX were then added to the bacterial suspension to a concentration of 10 μM, respectively. All groups were incubated in the dark at 37 °C for 30 min, and washed three times with PBS. Then the fluorescence was measured by CLSM (TCS SP8 STED 3x).

2.2.4 Live/dead fluorescent staining of bacterial cells. *S. aureus* and *E. coli* (1×10^5 CFU/mL) were incubated with 1 μM of KLA, PpIX and PPK. After incubation in the dark at 37 °C for 30 min, the bacteria treated with PpIX and PPK were exposed to 660 nm light (30 mW/cm^2, 10 min). After that, all experiments were harvested and washed with PBS for twice, then bacteria were stained with SYTO 9 and propidium iodide in the dark for 15 min. The fluorescence of the samples was observed with invert microscope.

2.2.5 Preparation of bacteria samples for SEM. The morphologies of the microorganisms before and after treatment with peptide were observed using a field emission scanning electron microscope (Sigma). After treatment as described above, the bacteria were dropped on a glass coverslip. The coverslips were finally dried then mounted and sputter coated with gold-palladium.

2.2.6 Hemolysis Assays. Blood samples were collected from healthy BALB/c mice, and washed with PBS three times to obtain blood cells, equal numbers of blood cells in PBS were mixed with different concentration of KLA, PpIX and PPK, and incubated in tubes at 37 °C. Each measurement was conducted in triplicate. The hemoglobin release was monitored at 541 nm by a microplate reader (Bio-Rad, model 550, USA). The red blood cell suspension in PBS was used as negative control. RBCs treated with 0.1% Triton X-100 was used as positive control for 100% lysis. Percent hemolysis was calculated as

(OD_{541}sample-OD_{541}negative)/(OD_{541}positive-OD_{541}negative) ×100%.

2.3. *In vivo* antimicrobial assay

2.3.1 Animals and infected model. BALB/c nude mice (5-week old) were bought from Wuhan University Animal Biosafty Level III Lab. All animal studies were approved by the Institutional Animal Care and Use Committee (IACUC) of the Animal Experiment Center of Wuhan University (Wuhan, China). All mouse experimental procedures were performed in accordance with the Regulations for the Administration of Affairs Concerning Experimental Animals approved by the State Council of People's Republic of China. Each mouse was created one subcutaneous infection site by injecting a dose of *S. aureus* (1×10^8 CFU/μL) in the right flank of mice to initiate infection.

2.3.2 *In vivo* fluorescence imaging. Two days after subcutaneous injection of *S. aureus* (1×10^8 CFU/μL), infected mice were randomly divided into two groups. All mice were intravenous injection with PpIX and PPK solutions (500 μM, 100 μL) respectively, at 0.5 h, 1 h, 2 h, 4 h, 6 h, 8 h, 12 h and 24 h after injection, mice were anesthetized and imaged by the IVIS Spectrum (Perkin Elmer) using the excitation wavelength of 640 nm and fluorescence emission signal wavelength of 700 nm. Then, mice were sacrificed for tissue distribution study after 24 h, including the infected tissue, heart, liver, spleen, lung and kidney.

2.3.3 *In vivo* photodynamic therapy of bacteria. Two days after subcutaneous injection of *S. aureus* (1×10^8 CFU/μL), infected mice were randomly divided into PBS, KLA, PpIX, PpIX+L, PPK, PPK+L groups. The remaining six groups were separately intravenous injection with PBS, KLA, PpIX and PPK solutions (500 μM, 100 μL). PDT treatment was conducted on PpIX and PPK groups by irradiating the subcutaneous infection site with NIR irradiation (660 nm, 30 mW/cm^2, 5 min). To observe the impact of peptide on blood and evaluate the therapeutic effects, mice blood was collected before sacrificed and measured with an auto hematology analyzer (MC-6200Vet, Icubio, China). Then the major organs (heart, liver, spleen, lung and kidney) and subcutaneous infection site were excised and collected for further analysis.

2.3.4 Histology. For histology, the major organs and subcutaneous infection site treated with different conditions were fixed in 4% paraformaldehyde PBS buffer and stained with H&E and FISH (Fluorescence in situ hybridization). The samples were examined in Wuhan Google Biotechnology Co., Ltd.

3. Results and discussion

3.1 Synthesis and characterization of PPK

In this investigation, the positively charged and α-helical proapoptotic peptide KLA was used to enhance the interaction with negatively charged bacterial membrane and further disrupt it. Then the hydrophobic photosensitizer PpIX was conjugated to KLA by using the short-chain PEG as a hydrophilic linker to improve the solubility. The KLA and chimeric peptide PPK were synthesized by a standard fluorenylmethyloxycarbonyl (Fmoc) solid-phase peptide synthesis (SPPS) method.[30] The synthesis process was detailedly described in the experimental section (Figure S1). The molecular weights of PPK and KLA were determined by electrospray ionization mass spectrometry (ESI-MS, Figure S2). As validated by the UV-vis spectra (Figure 1A), a Soret band at 400 nm was found for PPK, demonstrating that PPK did not change its UV-visible absorption significantly in comparison with PpIX.[32] As shown in Figure 1B, fluorescence intensities of PPK and PpIX were measured from 450 nm to 700 nm. Next, the ROS generation was tested by using dichlorofluorescein (DCFH). The fluorescence of DCFH will be increased in the presence of different concentrations of ROS. Under 660 nm light (30 mW/cm^2, 10 min), DCFH exhibited gradually increased fluorescence owing to the ROS generation of PPK (Figure 1C). It is known that the biological activity of KLA is dependent on the specific α-helical conformation. Therefore, the Fourier transform infrared spectroscopy (FT-IR) spectrum was employed to examine the structure of PPK. As shown in Figure 1D, the absorbance of amide I at around 1658 cm^{-1} and 1542 cm^{-1} in the FT-IR spectra indicated that those peptides mainly adopted the α-helical conformation.[33] To identify the positive charge property, zeta potential of KLA, PpIX and PPK was vaulted in phosphate buffer solution (PBS, pH 7.4) and it changed from -19.2 mV (PpIX) to 19 mV (PPK) (Figure S3).

3.2 *In vitro* antibacterial activity evaluation

The antibacterial activity of KLA, PpIX and PPK was evaluated by using Gram-negative *E. coli* and Gram-positive *S. Aureus* via the spread plate method. These three different samples (KLA, free PpIX and PPK) were incubated with *E. coli* and *S. aureus* with a

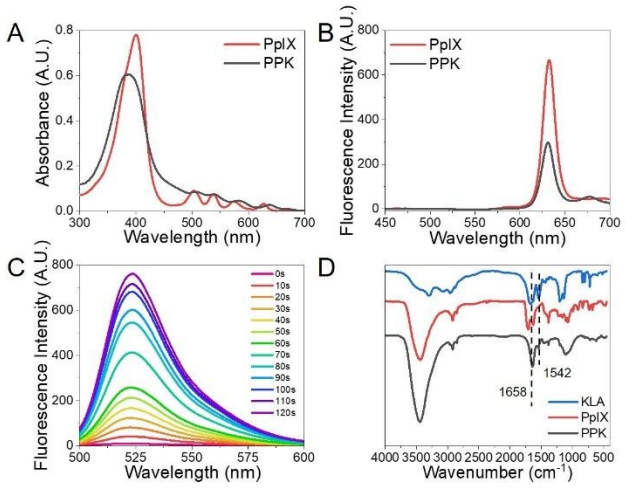

Figure 1. A) UV-vis spectrum of PpIX and PPK (1×10^{-4} M) in PBS. B) Fluorescence emission spectra of PpIX and PPK (1×10^{-4} M). C) Fluorescence intensity of DCFH indicate the generation of ROS by PPK (1×10^{-4} M) after 660 nm light (30 mW/cm^2, 10 min) for different time periods. D) FT-IR spectrum of KLA, PpIX and PPK, The characteristics absorption bands at 1658 cm^{-1} and 1542 cm^{-1} indicated that those peptides mainly adopted α-helical conformation.

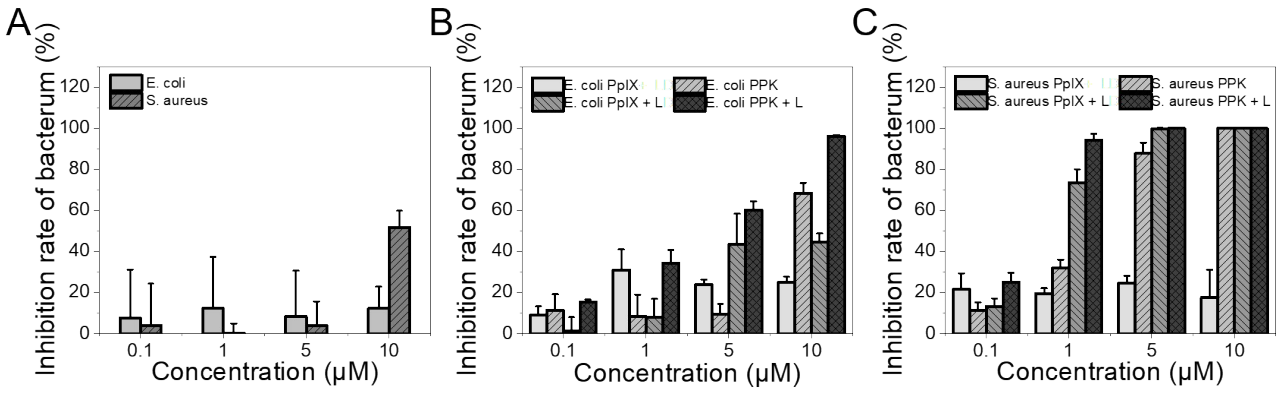

Figure 2. A) Inhibition rate of *E. coli* and *S. aureus* treated with KLA. Inhibition rate of B) *E. coli* and C) *S. aureus* treated with PpIX and PPK with/without 660 nm light (30 mW/cm^2, 10 min).

series of concentrations (0.1-10 μM) under same irradiation time (30 mW/cm^2, 10 min). As shown in Figure 2A, KLA showed negligible antibacterial effect on both *E. coli* and *S. aureus* even when the concentration of KLA was increased to 5μM. The survival rate of these two bacteria was found to decrease with an increase of the concentration of each group. As shown in Figure 2B, *E. coli* treated with PpIX showed no obvious inhibition in the absence of light. Once irradiated with 660 nm light (30 mW/cm^2, 10 min), the survival rate of *E. coli* decreased to about 60% at the concentration of 10 μM owing to toxic ROS generation. Comparatively, an obviously higher antibacterial activity against *E. coli* was observed in the PPK group than the PpIX group in the absence or presence of light, resulting from the specific *E. coli* cell membrane binding and disrupting ability of the positively charged and α-helical peptide KLA. Moreover, the antibacterial efficiency of the PPK group treated with light was stronger than that without light owing to the precise ROS generation at the bacterial membrane domain. Besides, the antibacterial efficiency of PPK against Gram-positive *S. aureus* was also studied. As shown in Figure 2C, PPK exhibited 94% inhibition rate of *S. aureus* even with the extremely low concentraion of 1 μM under light irradiation, which was obviouly stronger than the free PpIX group. All these results indicated that PPK displayed a more efficient antibacterial effect than the free PpIX both for Gram-positive and Gram-negative bacteria strains. Moreover, there was obviously different antibacterial effect of the free PpIX and PPK against *E. coli* and *S. aureus* due to their distinct cell walls. The cytoplasmic membrane of Gram-positive bacteria was surrounded by a relative porous layer of peptidoglycan and lipoteichoic acid, and it allowed the entry of photosensitizers and the insertion of chimeric peptide,[34] thus exhibiting the remarkable antibacterial effect. However, general PSs inculding the free PpIX bind only to the outer membrane of Gram-negative microorganisms and

View Article Online
DOI: 10.1039/C8TB02942D

result in negligible antibacterial effect. But positive-charged chimeric peptide PPK could facilitate the binding to the constituents of the Gram-negative bacterial membrane by electrostatic interactions and insertion, leading to the destabilization of the native organized membrane[35,36] by diffusing into the bacteria and generating ROS under light irradiation for enhanced antibacterial effects. These results are consistent with the previous reports but more efficient than before.[37, 38] Moreover, with a series of concentrations (0.1-10 μM), the toxicity of KLA, PpIX and PPK to 3T3 cells was tested, and negligible toxicity effect of PPK was observed in the absence of 660 nm light, but a notable cytotoxicity to 3T3 cells was observed in the presence of 660 nm light (Figure S4).

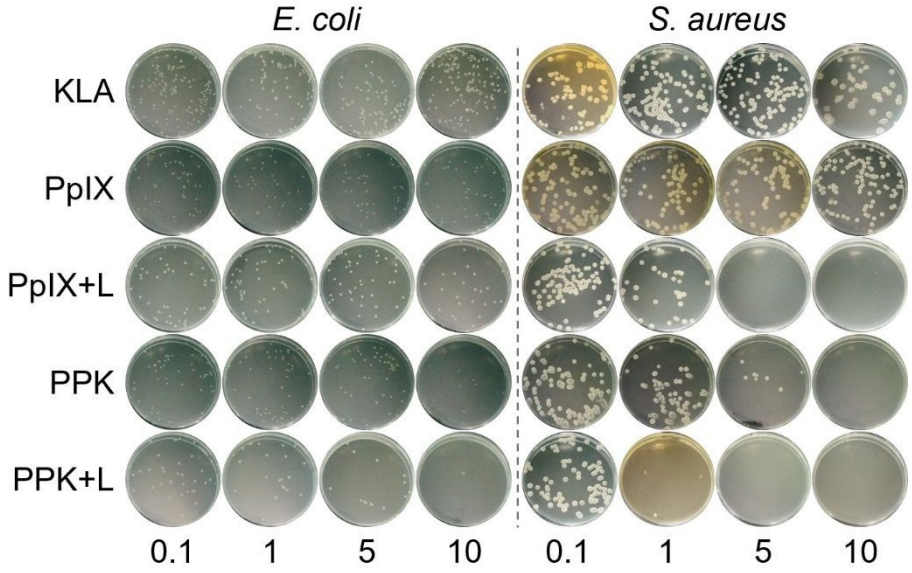

Figure 3. The colony forming units on LB agar plate of *E. coli* and *S. aureus* treated with KLA, PpIX and PPK at different concentrations (0.1 - 10 μM) with/without 660 nm light (30 mW/cm², 10 min).

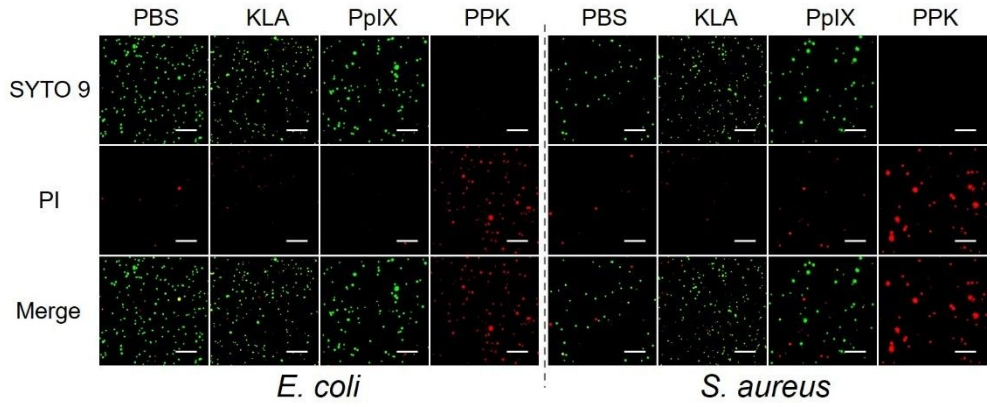

Figure 4. Live/dead fluorescent bacterial staining of *S. aureus* and *E. coli* treated with KLA, PpIX and PPK with 660 nm light (30 mW/cm², 10 min). Scale bar: 100 μm.

Afterward, the antibacterial effects were also observed in the spread plate assay. As shown in Figure 3, the growth inhibition of two bacterial stains was negligible with KLA at a series of concentration (0.1-10 μM). Combining with the results mentioned above, the colony forming units of *S. aureus* were inhibited with PpIX under the light but unconspicuous in *E. coli*. Under the same conditions, the colony forming units of both *S. aureus* and *E. coli* were obviously inhibited by PPK treated with light, indicating that PPK possessed a broad spectrum of antibacterial activity against microbial pathogens.

A live/dead staining assay was carried out to further assess the antibacterial activity of PPK. The bacteria treated with PBS were as control. As shown in Figure 4, there was an obvious difference in the fluorescence of both *S. aureus* and *E. coli* treated with KLA, PpIX and PPK (1μM) under 660 nm light. With KLA and PpIX treatment, most of green fluorescence was detected, indicating that most bacteria were alive. In contrast, under the treatment of PPK, the majority of red fluorescence was visualized and little green fluorescence was observed,

View Article Online
DOI: 10.1039/C8TB03004D

which suggested that bacteria were eliminated by PPK under 660 nm light (30 mW/cm^2, 10 min).

3.3 *In vitro* antibacterial mechanism study

As above mentioned, the introduction of cationic KLA is helpful in the binding of PPK to the outer wall of Gram-positive and Gram-negative bacteria. Thus, the bacterial membrane binding by PPK was confirmed by confocal laser scanning microscopy (CLSM). *S. aureus* and *E. coli* were incubated with PPK and PpIX for 30 min, respectively. The results were shown in Figure 5. The bacteria incubated with PpIX did not exhibited any fluorescence signal. In sharp contrast, both Gram-positive and Gram-negative bacteria treated with PPK showed strong fluorescence signals, demonstrating the excellent bacterial membrane targeting and binding by the cationic and α-helical proapoptotic peptide KLA.

To further verify the bacterial membrane damage by PPK, SEM was employed to visualize the bacterial membrane structure and morphology after treated with PPK. As can be seen from Figure 6, *E. coli* in PBS showed regular shape with clear borders and bacterial membrane, but wrinkled and shriveled *E. coli* were observed after light with PPK, owing to partial damage of the bacterial membrane with release of cytoplasmic contents. The same results were obtained for

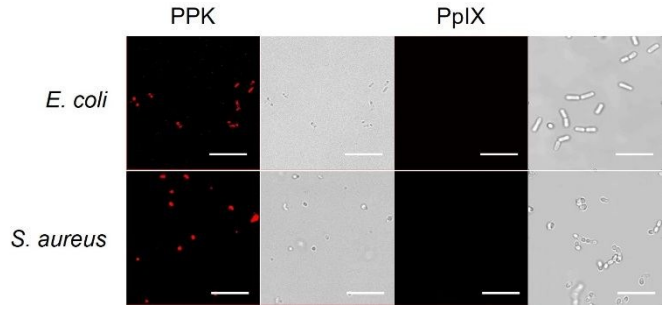

Figure 5. Confocal laser scanning microscopy (CLSM) images of *S. aureus* and *E. coli* incubated with 10 μM PPK and PpIX respectively for 30 min. Ex, 405 nm, Em, 630 nm. Scale bar: 10 μm.

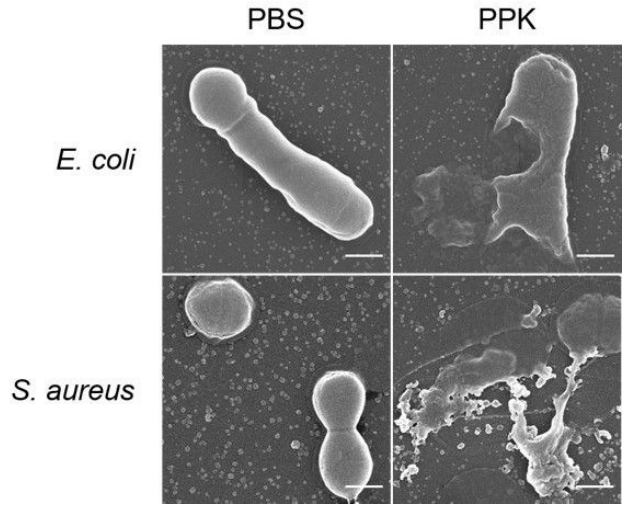

Figure 6. SEM photographs of bacteria treated with PBS and PPK under 660 nm light (30 mW/cm^2, 10 min). Scale bar: 500 nm.

S. aureus before and after treated with PPK. *S. aureus* treated with PBS was in spherical shape. After the treatment mentioned above, leakage of inner contents and irregular shape of *S. aureus* was observed, indicating severe damage of *S. aureus* caused by PPK. Leakage of the cellular component further justified that the bacterial membrane was the major damaged location caused by PPK.

These results demonstrated that bacteria treated with PPK exhibited a significantly enhanced photodynamic cytotoxicity compared with PpIX. The positive charge and α-helical conformation facilitated the binding to the bacteria membrane, the disrupting of membrane and subsequent oxidation of lipid bilayer mediated by the ROS, providing an enhanced photodynamic antibacterial activity.

3.4 *In vivo* fluorescence imaging

Before the evaluation of the photodynamic therapy effect, the accumulation effect of PPK at the infected tissues was first studied in a *S. aureus*-infected mice model using *in vivo* fluorescence imaging. The mice were intravenously injected with PpIX or PPK, respectively, and then imaged by a small animal imaging system at different time points. As shown in Figure 7A, for the mice injected with PpIX, there is no obvious fluorescence signal in the subcutaneous infection site. However, after injected with PPK, fluorescence intensity at infection site increased gradually and the strongest signal was observed at 6 h post-injection. After 24 h injection, the fluorescence signal at infected site was still strong, indicating the long-term retention effect and promising antibacterial potential of PPK. To image and quantify the fluorescence intensity in infected tissue and other organs for biodistribution analysis, the mice were sacrificed at 24 h post-injection. The infected mice injected with PpIX only exhibited fluorescent signal at the infected tissue. Notably, the subcutaneous infection site in the infected mice treated with PPK exhibited distinct fluorescent signal, and the fluorescence intensity was much higher than that of the mice treated with PpIX. What is more, quantitative analysis of the fluorescence intensity in various organs also confirmed this result (Figure 7B, C).

3.5 Antibacterial efficiency on *S. aureus*-infected mice model

According to the promising antibacterial effect *in vitro* and favorable accumulation in infected tissues, the *in vivo* therapeutic effect was evaluated by the chimeric peptide PPK. After subcutaneous injection of *S. aureus* (1×10^8 CFU/μL) for two days, infected mice were randomly divided into six groups, and conducted with different treatments as follows: PBS, KLA, PpIX, PpIX+L, PPK and PPK+L, respectively. The photos of the infected tissues were obtained after 7 days. Obviously, the infected wound was nearly healed in PPK+L group compared with the large infected sites in other groups (Figure 8A). Then, the mice were sacrificed for collecting major organs and infected tissues, and aliquots of diluted homogenized infected tissues of each group were plated on the LB agar. As shown in Figure 8B, the colony forming units in PPK+L group were much less than other groups. Moreover, the results of histological analysis of infected tissues showed less inflammatory cells emerged on the wound in the PPK+L group, while a large

View Article Online
DOI: 10.1039/C8TB03094D

amount of inflammatory cells appeared on the wound in other groups (Figure 8C). Fluorescence in situ hybridization (FISH) was used to observe the content of bacteria (red). A large quantity of red fluorescence was observed in the groups of PBS, KLA, PpIX, PpIX+L and PPK. However, the PPK+L group showed obviously decreased red fluorescence (95%) compared with the other five groups (Figure 8D). These results demonstrated that PPK could effectively kill bacteria under light irradiation. We also evaluated the systemic toxicity of these treatments, and the H&E staining results of the major organs (heart, liver, spleen, lung and kidney) exhibited no obvious impact on the major organs (Figure S5). Afterward, the biocompatibility and biosafety of PPK was tested *in vivo*. As shown in Figure S6, it is concluded that RBCs can remain minimal hemolysis in the presence of PPK (up to 50 μM). Moreover, the impact of PPK on blood was evaluated by the blood biochemistry and hematologic analysis, and no long-term side effects of PPK could be found (Figure S7). These results suggested the good biocompatibility and biosafety of PPK.

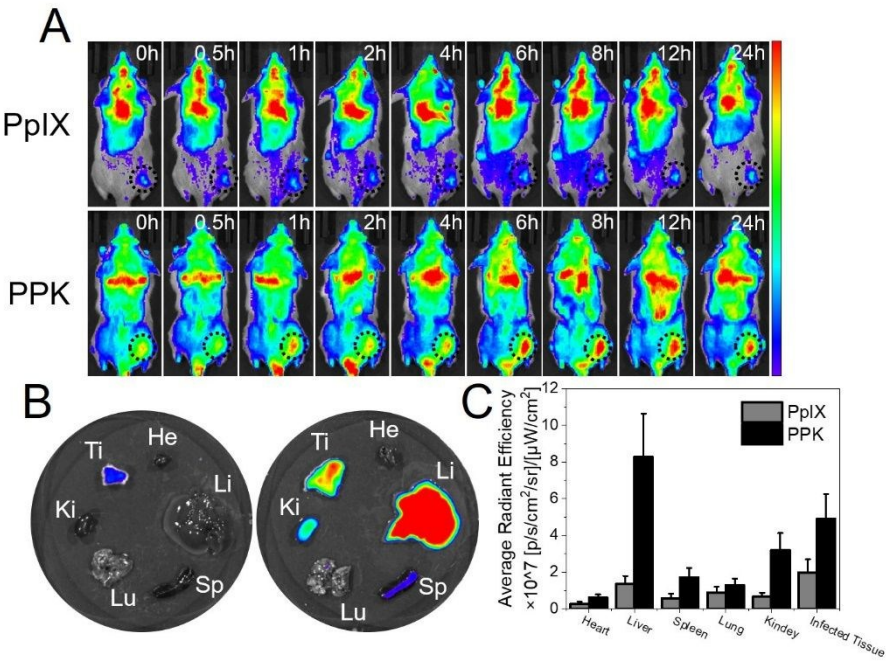

Figure 7. (A) Fluorescence images of S. aureus-infected mice after the intravenous injection of PpIX or PPK (500 μM) at different time points; (B) Ex vivo imaging of major organs; (C) The corresponding mean fluorescence intensity of infected tissue and major organs at 24 h post-injection.

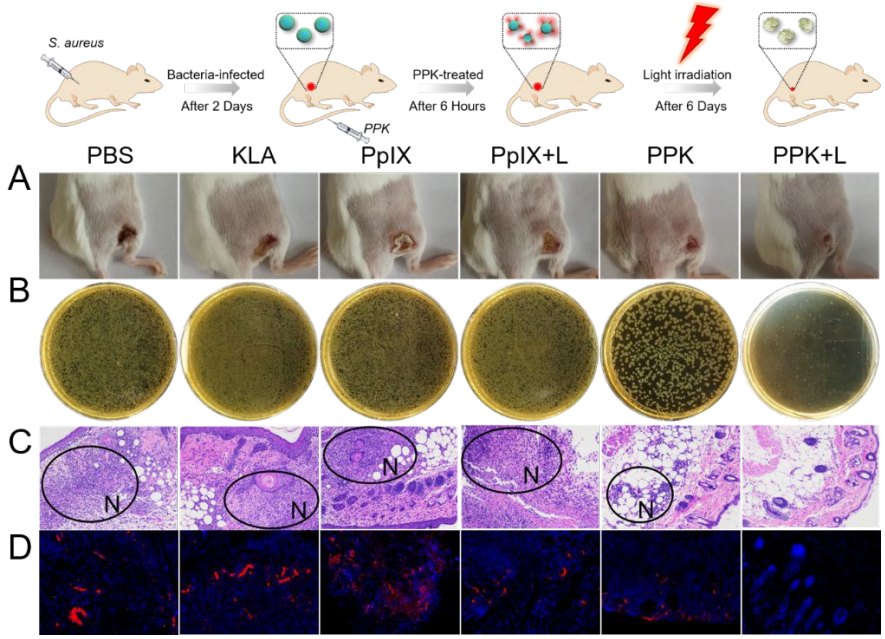

Figure 8. The images of A) Infected wound after 7 days of treatment by PBS, KLA, PpIX, PpIX + L, PPK and PPK + L. B) The LB agar of aliquots of diluted homogenized infected tissue. C) H&E staining images of the infected tissues with different treatments. D) Fluorescence in situ hybridization (FISH) of the infected tissues with different treatments.

4. Conclusions

To sum up, a biocompatible and biosafety antibacterial peptide PPK was prepared to treat bacterial infection by PDT. In this research, the chimeric peptide PPK could target to the bacterial membrane, then cause membrane damage and liposomal leakage. Moreover, the efficient ROS generation at the bacterial membrane domain led to the enhanced antibacterial effect both *in vivo* and *in vitro*. The results revealed that PPK possessed great antibacterial activity against both Gram-positive and Gram-negative bacteria under a short irradiation time, and reached more than 95% antibacterial effect in bacterial infected murine model. This bacterial membrane-binding photodynamic antibacterial strategy achieved highly efficient bacterial inhibition both *in vivo* and *in vitro*. Overall, we expected that the PPK developed in this study could be potential for the future photodynamic antimicrobial application.

Conflicts of interest

There are no conflicts to declare

Acknowledgements

This work was supported by the National Natural Science Foundation of China (51573142, 51690152 and 21721005) and CAS Interdisciplinary Innovation Team (Y7592911ZX).

References

1 J. M. A. Blair, M. A. Webber, A. J. Baylay, D. O. Ogbolu, L. J. V. Piddock, *Nat. Rev. Microbiol.*, 2015, **13**, 42-51.
2 F. Nederberg, Y. Zhang, J. P. K. Tan, K. Xu, H. Wang, C. Yang, S. Gao, X. D. Guo, Fukushima, K.; Li, L.; Hedrick, J. L.; Yang, Y. Y. *Nat. Chem.*, 2011, **3**, 409-414.
3 A. M. Durantini, D. A. Heredia, J. E. Durantini, E. N. Durantini, *Eur. J. Med. Chem.*, 2018, **144**, 651-661.
4 S. M. Dizaj, F. Lotfipour, M. Barzegar-Jalali, M. H. Zarrintan, K. Adibkia, *Mater. Sci. Eng. C*, 2014, **44**, 278-284.
5 S. Thamphiwatana, P. Angsantikul, T. Escajadillo, Q. Zhang, J. Olson, B. T. Luk, S. Zhang, R. H. Fang, W. Gao, V. Nizet, L. Zhang, *Proc. Natl. Acad. Sci. U.S.A.*, 2017, **114**, 11488-11493.
6 Hu, W.; Peng, C.; Luo, W.; Lv, M.; Li, X.; Li, D.; Huang, Q.; Fan, C. Graphene-Based Antibacterial Paper. *ACS Nano*, 2010, **4**, 4317-4323.
7 A. de Breij, M. Riool, R. A. Cordfunke, N. Malanovic, L. de Boer, R. I. Koning, E. Ravensbergen, M. Franken, T. van der Heijde, B. K. Boekema, P. H. S. Kwakman, N. Kamp, A. El Ghalbzouri, K. Lohner, S. A. J. Zaat, J. W. Drijfhout, P. H. Nibbering, *Sci. Transl. Med.*, 2018, **10**, eaan4044.
8 Z. Zhao, R. Yan, X. Yi, J. Li, J. Rao, Z. Guo, Y. Yang, W. Li, Y. Q. Li, C. Chen, *ACS Nano*, 2017, **11**, 4428-4438.
9 W. Kim, W. Zhu, G. L. Hendricks, D. V. Tyne, A. D. Steele, C. E. Keohane, N. Fricke, A. L. Conery, S. Shen, W. Pan, K. Lee, R. Rajamuthiah, B. B. Fuchs, P. M. Vlahovska, W. M. Wuest, M. S. Gilmore, H. Gao, F. M. Ausubel, E. Mylonakis, *Nature*, 2018, **556**, 103-107.
10 E. Alves, M. A. Faustino, M. G. Neves, Â. Cunha, H. Nadais, A. Almeida, *Photobiol. C-Photochem. Rev.*, 2015, **22**, 34-57.
11 R. E. W. Hancock, H. G. Sahl, *Nat. Biotechnol.*, 2006, **24**, 1551-1557.
12 G. B. Qi, D. Zhang, F. H. Liu, Z. Y. Qiao, H. Wang, *Adv. Mater.*, 2017, **29**, 1703461-1703471.
13 L. Misba, S. Kulshrestha, A. U. Khan, *Biofouling*, 2016, **32**, 313-328.
14 M. N. Urrutia, F. L. Alovero, C. S. Ortiz, *Dyes Pigment.*, 2015, **116**, 27-35.
15 F. Le Guern, V. Sol, C. Ouk, P. Arnoux, C. Frochot, T. S. Ouk, *Bioconjugate Chem.*, 2017, **28**, 2493-2506.
16 L. Y. Huang, A. El-Hussein, W. Xuan, M. R. Hamblin, *J. Photochem. Photobiol. B-Biol.*, 2018, **178**, 277-286.
17 C. M. Courtney, S. M. Goodman, J. A. McDaniel, N. E. Madinger, A. Chatterjee, P. Nagpal, *Nat. Mater.*, 2016, **15**, 529-535.
18 R. Dosselli, M. Gobbo, E. Bolognini, S. Campestrini, E. Reddi, *ACS Med. Chem. Lett.*, 2010, **1**, 35-38.
19 B. Wang, M. Wang, A. Mikhailovsky, S. Wang, G. C. Bazan, *Angew. Chem. Int. Edit.*, 2017, **129**, 5113-5116.
20 A. Parthasarathy, S. Goswami, T. S. Corbitt, E. Ji, D. Dascier, D. G. Whitten, K. S. Schanze, *ACS Appl. Mater. Interfaces*, 2013, **5**, 4516-4520.
21 C. F. Xing, Q. Xu, H. Tang, L. Liu, S. Wang, *J. Am. Chem. Soc.*, 2009, **131**, 13117-13124.
22 Y. Ma, Q. Mou, X. Zhu, D. Yan, *Mater. Today Chem.*, 2017, **4**, 26-39.
23 L. L. Li, G. B. Qi, F. Yu, S. J. Liu, H. Wang, *Adv. Mater.*, 2015, **27**, 3181-3188.
24 X. Yang, J. Yang, L. Wang, B. Ran, Y. Jia, L. Zhang, G. Yang, H. Shao, X. Jiang, *ACS Nano*, 2017, **11**, 5737-5745.
25 F. Liu, A. Soh Yan Ni, Y. Lim, H. Mohanram, S. Bhattacharjya, B. Xing, *Bioconjugate Chem.*, 2012, **23**, 1639-1647.
26 M. Sharma, L. Visai, F. Bragheri, I. Cristiani, P. K. Gupta, P. Speziale, *Antimicrob. Agents Chemother.*, 2008, **52**, 299-305.
27 H. R. Jia, Y. X. Zhu, Z. Chen, F. G. Wu, *ACS Appl. Mater. Interfaces*, 2017, **9**, 15943-15951.
28 S. A. Sieber, M. A. Marahiel, *Chem. Rev.*, 2005, **105**, 715-738.
29 X. L. Gao, W. Tao, W. Lu, Q. Zhang, Y. Zhang, X. Jiang, S. Fu, *Biomaterials*, 2006, **27**, 3482-3490.
30 C. Zhang, L. H. Liu, W. X. Qiu, Y. H. Zhang, W. Song, L. Zhang, X. B. Wang, X. Z. Zhang, X. Z. *Small*, 2018, **14**, 1703321-1703329.
31 K. Han, Q. Lei, S. B. Wang, J. J. Hu, W. X. Qiu, J. Y. Zhu, W. N. Yin, X. Luo, X. Z. Zhang, *Adv. Funct. Mater.*, 2015, **25**, 2961-2971.
32 G. F. Luo, W. H. Chen, S. Hong, Q. Cheng, W. X. Qiu, X. Z. Zhang, *Adv. Funct. Mater.*, 2017, **27**, 1702122-1702134.
33 W. H. Chen, X. D. Xu, G. F. Luo, H. Z. Jia, S. X. Cheng, R. X. Zhuo, X. Z. Zhang, *Sci Rep*, 2013, **3**, 3468-3474.
34 G. B. Kharkwal, S. K. Sharma, Y. Y. Huang, T. Dai, M. R. Hamblin, *Lasers Surg. Med.*, 2011, **43**, 755-767.
35 H. A. Sutterlin, H. Shi, K. L. May, A. Miguel, S. Khare, K. C. Huang, T. J. Silhavy, *Proc. Natl. Acad. Sci. U.S.A.*, 2016, **113**, E1565-E1574.
36 J. A. Jackman, H. Z. Goh, V. P. Zhdanov, W. Knoll, N. J. Cho, *J. Am. Chem. Soc.*, 2016, **138**, 1406-1413.
37 S. Meng, Z. Xu, G. Hong, L. Zhao, J. Guo, H. Ji, T. Liu, *Eur. J. Med. Chem.*, 2015, **92**, 35-48.
38 G. A. Johnson, N. Muthukrishnan, J. P. Pellois, *Bioconjugate Chem.*, 2012, **24**, 114-123.

Journal Name ARTICLE

TOC Image

View Article Online
DOI: 10.1039/C8TB03094D

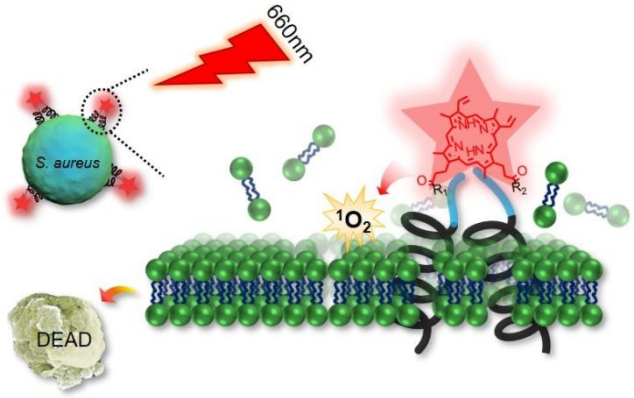

A versatile bacterial membrane-binding chimeric peptide PpIX-[PEG_8-$(KLAKLAK)_2$]$_2$ by conjugating a photosensitizer protoporphyrin IX with the antimicrobial peptide $(KLAKLAK)_2$ was constructed for effective photodynamic inactivation of bacteria.